NASA Contractor Report 181935
ICASE Report No. 89-76

ICASE

DIRECT DISCRETIZATION OF PLANAR div-curl PROBLEMS

R. A. Nicolaides

Contract No. NAS1-18605
October 1989

Institute for Computer Applications in Science and Engineering
NASA Langley Research Center
Hampton, Virginia 23665-5225

Operated by the Universities Space Research Association

National Aeronautics and
Space Administration

Langley Research Center
Hampton, Virginia 23665-5225

DIRECT DISCRETIZATION OF PLANAR div-curl PROBLEMS

R. A. Nicolaides[1,2]

Department of Mathematics
Carnegie Mellon University
Pittsburgh, PA 15213

ABSTRACT

A control volume method is proposed for planar div-curl systems. The method is independent of potential and least squares formulations, and works directly with the div-curl system. The novelty of the technique lies in its use of a single local vector field component and two control volumes rather than the other way round. A discrete vector field theory comes quite naturally from this idea and is developed in the paper. Error estimates are proved for the method, and other ramifications investigated.

[1]This research was supported by the National Aeronautics and Space Administration under NASA Contract No. NAS1-18605 while the author was in residence at the Institute for Computer Applications in Science and Engineering (ICASE), NASA Langley Research Center, Hampton, VA 23665.

[2]This work was supported by the United States Air Force under grant AFOSR 89-0359.

1 Introduction. Although div-curl systems occur in fluid dynamics, in electrodynamics and several other applications, relatively few discretizations are available. A possible reason is that equivalent potential formulations often exist. Another reason is that the simple minded Galerkin finite element approach is not convergent in general. A least squares formulation is the usual way to get a convergent finite element scheme for planar problems. The situation in three dimensions is worse. For example, the vector potential approach can have spurious mode problems [10]. Underlying the difficulties is the latent overdetermination of the div-curl system (4 equations, 3 unknown functions).

This article contains an alternative approach which works directly with the div-curl equations and does not involve potentials or least squares. The new recipe is finite volume based, but differs in a key ingredient. The change permits the development of a discrete vector analysis. In turn, this provides tools for analysis of the discretization and for other purposes.

Central to the approach is the use of dual pairs of meshes made up of "complementary volumes". In three dimensions, they have the property that the edges of each mesh are perpendicular to the faces of the other. There are many possibilities for such mesh pairs. In two dimensions, the simplest example consists of the staggered Cartesian meshes (MAC meshes) well known in fluid mechanics. The complementary volumes are the basic mesh squares and the shifted mesh squares centered on the nodes of the basic mesh. For triangular and tetrahedral meshes, an example is given by Voronoi-Delaunay mesh pairs. Many other possibilities exist, including prismatic meshes in three dimensions and combinations of these meshes.

The basic idea of the discretization is to define field components along the edges of one of the meshes, and, therefore, normal to the faces of the other. In two dimensions, this single component is enough to permit the definition of two field operators corresponding to div and curl. With boundary conditions, these are sufficient to define the discrete field. Associated with the nodes of the two meshes are the two discrete potentials which generate the null spaces of the discrete div and curl. The usual relations are valid between these operators and potentials.

We will address only the two dimensional problem in this paper. The main ideas go over naturally to three dimensions but are sufficiently different to warrant a separate treatment. It will be given in a forthcoming report. The goals here are to provide a framework for error estimation of complementary volume schemes, and to develop the main tools of the discrete vector field theory.

In sections 2 and 3 the class of meshes of interest is specified, and a typical discretization is derived. Sections 4 and 5 contain the formulation and properties of the discrete vector field theory and some applications. Sections 6-8 are concerned with the main results of the error analysis. Section 7 in particular establishes a link with finite elements and applies the previous results to

error estimate a potential theory problem. Section 9 discusses special topics concerning rectangular meshes. Section 10 extends the results to more general boundary conditions.

The discretization technique reported here has significant extensions to higher order systems of partial differential equations, particularly to viscous fluid flow problems. Algorithms for the Navier-Stokes equations are provided in [4] and [7].

2 Locally Equiangular Meshes. We begin by defining a class of meshes of interest. Let Ω denote a bounded polygonal region of R^2. Ω may be multiply connected. Let Γ_0 denote the outer boundary, let $\Gamma_i \;\; i = 1, 2, \ldots, r$ denote the inner (polygonal) boundaries if they exist and let $\Gamma := \cup_{i=0}^{r} \Gamma_i$. $\Gamma_i \;\; i = 1, 2, \ldots, r$ are considered to bound "holes" $\Omega_i \;\; i = 1, 2, \ldots, r$. Ω will be triangulated and a dual tesselation will also be used. Let τ denote a triangulation of Ω with T triangles denoted by $\tau_i \;\; i = 1, 2, \ldots, T$ with N nodes $x_i \;\; i = 1, 2, \ldots, N_1 \in \Omega$ and $x_j \;\; j = N_1 + 1, N_1 + 2, \ldots, N \in \Gamma$ as well as E edges $\sigma_i \;\; i = 1, 2, \ldots, E_1 \in \Omega$ (*interior* edges) and $\sigma_j \;\; j = E_1 + 1, E_1 + 2, \ldots, E \in \Gamma$ (*boundary* edges). Two triangles are called *adjacent* if they share a common side. Then we can construct a dual tesselation by joining the circumcenters of adjacent triangles. Many duals of a given triangulation can be constructed. For example, another one could be made by joining the centroids of adjacent triangles. The dual which is based on circumcenters is rather special and will be called the *normal* dual since if two triangles are adjacent, the line joining their circumcenters is normal to (and bisects) their common side. The dual figures are polygons and in general they can have self intersecting boundaries. They will be called *covolumes*. The covolume associated with an interior node is the polygonal figure obtained by joining (in order) the circumcenters of the adjacent triangles which share it.

We will associate a (boundary) covolume with each boundary node as well. The procedure is illustrated in Figure 1, where the covolume for the boundary node A is the interior of the polygon PATSRQ.

In Figure 1 Q,R, and S are the circumcenters of their triangles, and P and T are the midpoints (and circumcenters) of their edges which are on Γ .

The normal dual, consisting of T nodes, E edges and N covolumes is denoted by τ'. Sometimes, we will use the "co" prefix to denote various elements of the normal dual, for example in referring to coedges, comesh and so on.

There is additional complexity associated with self intersecting covolumes which we wish to avoid. To do so, we require that τ is "locally equiangular" [8]:

Definition. *A triangulation is* locally equiangular *iff for every pair of adjacent triangles which form a convex quadrilateral, the sum of the angles opposite the common side is at most 180 deg.*

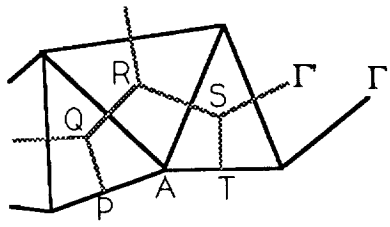

Figure 1:

Elementary geometry shows that if τ is locally equiangular then (1) each interior covolume is convex and (2) distinct covolumes have empty intersection and each point of Ω is either in a covolume or on the common boundary of two covolumes. Then τ' has inner and outer coboundaries Γ' consisting of those coedges which intersect edges of τ with just one node on Γ. These will be denoted by Γ'_0, and Γ'_i $i = 1, 2, \ldots, r$ when the latter exist. The section QRS in Figure 1 is part of Γ'. Note that any part of Γ' might penetrate the corresponding part of Γ . This will happen if there are obtuse angles opposite an edge of Γ, even if τ is locally equiangular.

We will obtain the results assuming that $r > 0$. The modifications for $r = 0$ are mostly self evident.

The two tesselations τ and τ' are close to being a Delaunay-Voronoi pair. However, although a Delaunay triangulation is always locally equiangular, the converse is false, at least when the classical definition of the Voronoi diagram is used. The problem occurs at boundaries. Recall that a standard Delaunay triangulation is defined by joining adjacent vertices if their Voronoi figures share a common edge. Then it follows that the Delaunay triangulation is a triangulation of the *convex hull* of the vertices. Since Ω is not convex in general, constructing the Delaunay triangulation of the vertices of τ does not necessarily give a triangulation of Ω . For the purposes of this article these distinctions are unimportant. Local equiangularity is the only property we need since all the properties required can be derived from it.

Some of the results below must be modified for certain kinds of trivial triangulations, in particular those with no interior triangles. We will always assume that the triangulations are sufficiently fine for the purposes at hand. No significant loss of generality is incurred by this assumption.

We will make frequent use of the following special case of Euler's formula:

Lemma 2.1. *Let τ denote a plane triangulation with N vertices, T triangles,*

E edges, and r holes. Then

$$N + T = E + 1 - r.$$

Proof. If $r = 0$ the lemma is easily proved by deleting triangles from τ while maintaining a count of N, T and E. If $r > 0$ we can imagine the holes triangulated consistently with τ . This gives a triangulation say $\bar{\tau}$ without holes. Combining the already established result for $\bar{\tau}$ and for the triangulations of the holes, the result follows by subtraction. □

3 Div-Curl Systems. One div-curl system of interest is

$$\operatorname{div} \mathbf{u} = \rho \qquad \text{in } \Omega \tag{1}$$

$$\operatorname{curl} \mathbf{u} = \omega \qquad \text{in } \Omega \tag{2}$$

$$\mathbf{u} \cdot \mathbf{n} = f \qquad \text{on } \Gamma \tag{3}$$

$$\int_{\Gamma_i} \mathbf{u} \cdot \mathbf{t}\, ds = \gamma_i \qquad i = 1, 2, \ldots, r \tag{4}$$

where $\vec{u} := (u, v)$, curl $\mathbf{u} := v_x - u_y$, $\mathbf{t}$ denotes the positively oriented unit tangent, $\mathbf{n}$ the outward unit normal, and it is assumed that

$$\int_\Omega \rho\, dx\, dy = \int_\Gamma f\, ds. \tag{5}$$

Also assumed is that $\rho \in L^2(\Omega)$, $\omega \in L^2(\Omega)$ and $f \in H^{1/2}(\Gamma)$ and that the system has a unique solution $\mathbf{u} \in \mathbf{H}^1(\Omega)$. See [6],[9] for information on this point. We will explain the basic ideas of the discretization in terms of (1)-(4). Section 10 extends the results to other boundary conditions.

Referring to Figure 2, we approximate (1) by

$$u_1 h_1 + u_2 h_2 + u_3 h_3 = \int_\Omega \rho\, dx\, dy. \tag{6}$$

Here and below, the u_j denote approximations to $\mathbf{u} \cdot \mathbf{n}_j$, $\mathbf{n}_j$ denote unit normals directed outwards and $h_j > 0$ denote the ordinary side lengths of τ. There will be a similar equation for each one of the T triangles in τ . In matrix form, with u denoting the vector of components u_j, these *flux* equations can be written as

$$Fu = \bar{\rho} \tag{7}$$

where $u \in R^E$ and $\bar{\rho} \in R^T$. Analogous to (6) discrete fluxes from the holes are also defined and we denote them by

$$F(u; \Gamma_j) \qquad j = 1, 2, \ldots, r.$$

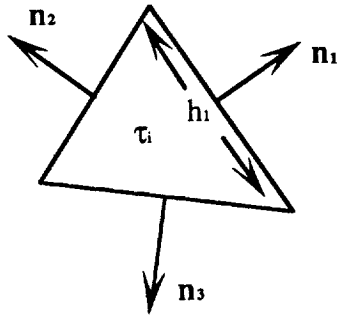

Figure 2:

For any $u \in R^E$, it is also convenient to introduce the $r \times E$ matrix $\mathcal{F}$ and denote the hole fluxes by $\mathcal{F}u$.

To approximate (2) we integrate it over an interior covolume $\tau_i' \in \tau'$ as illustrated in Figure 3. The arrows on the covolume edges denote the directions of

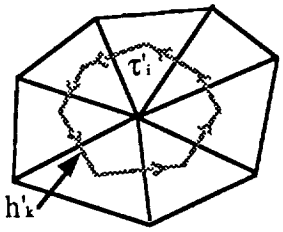

Figure 3:

the unit normals to the associated triangle edges. Approximation of the integral

$$\int_{\partial\tau_i'} \mathbf{u} \cdot \mathbf{t}\, ds \qquad (= \int_{\tau_i'} \text{curl } \mathbf{u}\, dx\, dy)$$

where $\partial\tau_i'$ denotes the positively oriented boundary and $\mathbf{t}$ the unit tangent gives

$$\sum_k u_k h_k' = \int_{\tau_i'} \omega\, dx\, dy \tag{8}$$

where the sum is over the coedges of $\partial\tau_i'$ and $h_k' \geq 0$ denotes the length of a coedge. Assembling these *circulation* equations gives the matrix equation

$$C_0 u = \bar{\omega} \tag{9}$$

where $u \in R^E$ and $\bar{\omega} \in R^{N_1}$. The zero subscript is intended to suggest that circulations in (9) are computed for interior nodes only. Discrete circulations around the hole coboundaries are defined similarly to (8) and denoted by

$$C(u;\Gamma_j') \qquad j = 1, 2, ..., r.$$

These circulations will be represented as $\mathcal{C}u$ where $u \in R^E$ and $\mathcal{C}$ is $r \times E$. The boundary condition (3) is discretized by defining boundary edge values for u by

$$u_k = \frac{1}{h_k} \int_{\sigma_k} f \, ds \qquad k = E_1 + 1, \ldots, E. \tag{10}$$

Note that there are $N - N_1$ of these equations.

The prescribed circulations (4) are approximated as

$$\begin{aligned} C(u;\Gamma_j') &= \gamma_j + \int_{s_j} \omega \, dx \, dy \qquad j = 1, 2, ..., r \\ &=: g_j \qquad j = 1, 2, ..., r \end{aligned} \tag{11}$$

where s_j denotes the strip lying between Γ_j and Γ_j'. We will assume that Γ_j' does not penetrate Γ_j to avoid extending ω outside Ω . This will hold iff opposite every triangle edge on Γ_j $j = 1, 2, \ldots, r$ is an acute angle. (No restriction is necessary for a simply connected domain). There is, of course, no assurance that a locally equiangular or even a Delaunay triangulation has no obtuse angles.

Equations (7),(9),(10) and (11) are a linear system of $T + N_1 + (N - N_1) + r = T + N + r$ equations in E unknowns. By Euler's formula there is one more equation than unknowns, so we expect a single constraint on the data. This will turn out to be

$$\sum_{\tau_i \in \tau} \bar{\rho}_i = \sum_{\sigma_j \in \Gamma} \bar{f}_j \tag{12}$$

which holds by (5). We will prove in section 5 that these discrete equations indeed have a unique solution.

4 Mesh Matrices. In this section some basic properties of dual mesh systems are derived. These will lead in the next section to a more detailed formulation of the equations in section 3. Similar results are valid for more general mesh systems than plane triangulations but will not be needed below.

Let τ denote an arbitrary triangulation of Ω with T triangles, E edges including E_1 interior edges and N nodes of which N_1 are interior nodes. Label the interior nodes $1, 2, \ldots, N_1$, the interior edges $1, 2, \ldots, E_1$ and assign the positive direction along each edge σ_k $k = 1, 2, \ldots, E$ to be from lower to higher node number. Let τ' denote a dual mesh, with T nodes E edges and N covolumes. The dual can be quite general, subject to having exactly one node in each triangle. The

dual edges obtained by joining adjacent dual nodes are in a biunique correspondence with the edges of τ. For each boundary triangle, we join the dual node to a point on the triangle's boundary. The dual edge corresponding to σ_k is denoted by σ'_k. For orienting the edges of τ' we use the convention that (σ'_k, σ_k) are oriented like a Cartesian coordinate system in the plane. This convention applies to both interior and boundary edges.

Denote by D the $E \times N$ edge-node incidence matrix of τ, where

$$D_{ij} := \begin{cases} +1 & \text{if } \sigma_i \text{ is directed into node } j \\ -1 & \text{if } \sigma_i \text{ is directed out of node } j \\ 0 & \sigma_i \text{ does not meet node } j. \end{cases}$$

D is easily seen to have rank $N-1$. Define D_0 to be the $E_1 \times N_1$ matrix obtained by deleting rows and columns of D corresponding to boundary edges and boundary nodes respectively. D_0 has rank N_1. If $r > 0$ we also define an $E_1 \times r$ matrix $\mathcal{D}$ as follows.

$$\mathcal{D}_{is} := \begin{cases} +1 & \text{if } \sigma_i \text{ is directed into } \Gamma_s \\ -1 & \text{if } \sigma_i \text{ is directed out of } \Gamma_s \\ 0 & \sigma_i \text{ does not meet } \Gamma_s. \end{cases}$$

In this, σ_i denotes interior edges, and $s = 1, 2, \ldots, r$. $\mathcal{D}$ has rank r.

For the dual τ' we define the $E \times T$ incidence matrix B as follows:

$$B_{ij} := \begin{cases} +1 & \text{if } \sigma'_i \text{ is directed out of } \tau_j \\ -1 & \text{if } \sigma_i \text{ is directed into } \tau_j \\ 0 & \sigma_i \text{ does not meet } \tau_j. \end{cases}$$

B has rank T. B_0 denotes B with rows corresponding to boundary edges deleted. B_0 is of order $E_1 \times T$. If $r > 0$ we define an $E \times r$ matrix $\mathcal{B}$ by

$$\mathcal{B}_{is} := \begin{cases} +1 & \text{if } \sigma'_i \text{ is directed out of } \Omega_s \\ -1 & \text{if } \sigma'_i \text{ is directed into } \Omega_s \\ 0 & \sigma'_i \text{ does not meet } \Gamma_s. \end{cases}$$

$\mathcal{B}$ has rank r.

An important result is the following:

Theorem 4.1. *Let $v \in R^{E_1}$. Then $\exists\, \phi \in R^T$ such that $v = B_0\phi$ iff $D_0^t v = 0$ and $\mathcal{D}^t v = 0$.*

Proof. Since $\operatorname{rank}(B_0) = T - 1$, we have

$$\begin{aligned} \dim N(B_0^t) &= E_1 - T + 1 \\ &= N_1 + r \end{aligned}$$

using lemma 2.1. Here and below, $N(\cdot)$ and $R(\cdot)$ denote the null space and range of their arguments. Next, it can be verified directly that $B_0^t D_0 \psi = 0 \forall \psi \in R^{N_1}$, and $B_0^t \mathcal{D} \xi = 0 \forall \xi \in R^r$, so that $R(D_0) \subset N(B_0^t)$ and $R(\mathcal{D}) \subset N(B_0^t)$. Direct verification also shows that $R(D_0) \cap R(\mathcal{D}) = 0$. Since $\dim R(D_0) + \dim R(\mathcal{D}) = N_1 + r$ it follows that $N(B_0^t) = R(D_0) \cup R(\mathcal{D})$. Solvability of the equation

$$B_0 \phi = v$$

holds iff

$$(v, z) = 0 \qquad \forall z \in N(B_0^t),$$

(,) denoting the standard Euclidean inner product. By the above, this is equivalent to

$$\begin{aligned} (v, D_0 \psi) &= 0 \qquad \forall \psi \in R^{N_1} \\ (v, \mathcal{D} \xi) &= 0 \qquad \forall \xi \in R^r, \end{aligned}$$

and these in turn are equivalent to the theorem. □

Corresponding to theorem 4.1 is:

Theorem 4.2. *Let $v \in R^E$. Then $\exists \psi \in R^N$ such that $v = D\psi$ iff $B^t v = 0$ and $\mathcal{B}^t v = 0$.*

Proof. Similar to theorem 4.1. □

5 Discrete vector fields. In this section we will express the flux and circulation operators in terms of the mesh properties of section 4 and develop some analogs of vector field theorems. For the remainder of the paper we will be using the normal dual exclusively. In any normal dual, the distance between two circumcenters will be zero if they coincide. Although this situation is "non-generic", it does occur in some situations (section 9). Other than this, it is assumed throughout that the circumcenters are all distinct. If, in fact, there are coincident circumcenters, the results obtained remain true, but minor variations in some proofs may be required. A second assumption, made throughout, is that the coboundary Γ' does not penetrate Γ. This was already mentioned in section 3 following (11).

In R^E introduce the inner product $[\cdot, \cdot]$ defined by

$$[u, v] := (u, HH'v) = (u, H'Hv) \tag{13}$$

and denote the associated norm by

$$\| u \|_W = [u, u]^{1/2}.$$

In (13) $H := \mathrm{diag}(h_k)$ and $H' := \mathrm{diag}(h'_k)$. Both H and H' are invertible and we let $W := HH'$. In Figure 4, ABC and ACD are adjacent triangles from τ,

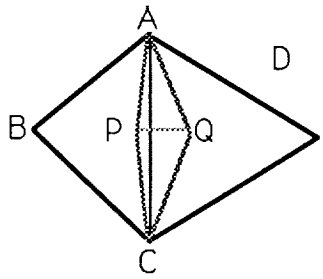

Figure 4:

and P and Q are their circumcenters. Let $|\ AC\ | := h_k$ and $|\ PQ\ | := h'_k$. The area of the *kite* shaped figure APCQ is $h_k h'_k/2$. The corresponding areas at boundaries are $h_l h'_l/4$. It follows that $\|\cdot\|_W$ is twice a discrete $L^2(\Omega)$ norm. This interpretation holds for any locally equiangular triangulation.

Denote R^E equipped with $[\cdot,\cdot]$ by $U \equiv U(\bar{\Omega})$. Then we can refer to "grid functions" $u \in U(\bar{\Omega})$ and regard them as having boundary values $u|_\Gamma$ and interior values $u|_\Omega$. Define

$$U_0 := \{u \in U\ ;\ u|_\Gamma = 0\}.$$

The flux and circulation operators of section 3 can be expressed as

$$\begin{aligned} F &= B^t H \\ C_0 &= D_0^t H'_0 \\ \mathcal{C} &= \mathcal{D}^t H'_0 \\ \mathcal{F} &= \mathcal{B}^t H \end{aligned}$$

where H'_0 denotes the restriction of H' to interior edges.. Verification of these is by direct calculation. Note that orientations are automatically taken into account in this formulation. Difference operators are defined as follows:

$$\begin{aligned} S\phi &:= (H')^{-1} B\phi \qquad \forall \phi \in R^T \\ S_0\phi &:= (H'_0)^{-1} B_0\phi \qquad \forall \phi \in R^T \\ T\psi &:= H^{-1} D\psi \qquad \forall \psi \in R^N. \end{aligned}$$

We will the notation H_0 to denote the restriction of H to interior edges, and $W_0 := H_0 H'_0 = H'_0 H_0$. The theorems of section 4 translate into theorems about the existence of potentials for mesh functions u with $C_0 u = 0$ and $\mathcal{C}u = 0$ (velocity/scalar potential) and $Fu = 0$ and $\mathcal{F}u = 0$ (stream function/vector potential).

Theorem 5.1. *If $C_0 u = 0$ and $\mathcal{C}u = 0$ then there exists $\phi \in R^T$ such that*

$u = S_0\phi$. *Conversely, if* $u := S_0\phi$ *then* $C_0 u = 0$ *and* $Cu = 0$.

Proof. Use theorem 4.1 to prove the first part and direct substitution for the converse. □

For the stream function, the analogous result is:

Theorem 5.2. *If* $Fu = 0$ *and* $\mathcal{F}u = 0$ *then there exists* $\psi \in R^N$ *such that* $u = T\psi$. *Conversely, if* $u := T\psi$ *then* $Fu = 0$ *and* $\mathcal{F}u = 0$.

Proof. For the first part use theorem 4.2. The converse is easily proved by direct substitution. □

Note that the converses in these theorems furnish analogs to the vector identities "curl grad $\phi = 0$" and "div curl $\mathbf{u} = 0$".

Another useful result is:

Lemma 5.1. *For all* $u \in U$, $\phi \in R^T$ *and* $\psi \in R^N$ *we have*

$$(1) \quad [u, S\phi] = (Fu, \phi)$$
$$(2) \quad [u, T\psi] = (Cu, \psi).$$

Proof. (1). By definition of S

$$\begin{aligned} [u, S\phi] &= (u, HH'(H')^{-1}B\phi) \\ &= (B^t H u, \phi) = (Fu, \phi). \end{aligned}$$

The proof of (2) is similar.□

These are analogs of integration formulas. For example, the first is analogous to

$$\int_\Omega \mathbf{u}.\nabla\phi\, dx\, dy = -\int_\Omega \phi \,\mathrm{div}\,\mathbf{u}\, dx\, dy \qquad (\phi\,|_\Gamma = 0).$$

Another useful result following from above is an analog of the Helmholtz decomposition of vector fields. In general, this decomposition is for the subspace of $\tilde{U}_0 \subset U_0$ whose definition is:

$$\tilde{U}_0 := \{u \in U_0; Cu = 0 \text{ and } \mathcal{F}u = 0\}$$

Actually, since $u \in U_0 \Rightarrow \mathcal{F}u = 0$, this requirement in the definition is redundant. It is included to make explicit a symmetry in the hypotheses. Also, before computing Cu we must restrict u to interior edges. This point will arise several times below and also in connection with C_0. We will still denote the restriction by u, and without explicit mention each time. If $r = 0$, then $\tilde{U}_0 = U_0$ and the

decomposition is for U_0 itself. We also define the following subspaces of $\tilde{U}_0$:

$$\begin{aligned} \mathcal{Z}_0 &= \{u \in \tilde{U}_0;\ Fu = 0\} \\ \mathcal{W}_0 &= \{u \in \tilde{U}_0;\ C_0 u = 0\}. \end{aligned}$$

Now we have:

Theorem 5.3. *$\tilde{U}_0$ has the decomposition*

$$\tilde{U}_0 = \mathcal{Z}_0 \oplus \mathcal{W}_0,$$

which is orthogonal relative to $[\cdot, \cdot]$.

Proof. First, note that if $w \in \mathcal{W}_0$, then by theorem 5.1 and part (1) of lemma 5.1 $\forall z \in \tilde{U}_0$,

$$[z, w] = [z, S_0\phi] = [z, S\phi] = (Fz, \phi)\ \forall \phi \in R^T.$$

Hence, if z is orthogonal to $\mathcal{W}_0$, then $Fz = 0$ which implies $z \in \mathcal{Z}_0$. On the other hand, if some $z \in \tilde{U}_0$ satisfies $Fz = 0$ and also $C_0 z = 0$ then we have for some $\phi' \in R^T$

$$\begin{aligned} [z, z] &= [z, S\phi'] \\ &= (Fz, \phi') \\ &= 0 \end{aligned}$$

so that $z = 0$. This proves the result. □

As an application of theorem 5.4 we will prove that the discrete system of section 3 has a unique solution. These equations are

$$Fu \equiv B^t H u = \bar{\rho} \tag{14}$$

$$C_0 u \equiv D_0^t H_0' u = \bar{\omega} \tag{15}$$

$$\mathcal{C}u \equiv \mathcal{D} H_0' u = \bar{g} \tag{16}$$

$$\mathcal{I}u = \bar{f}. \tag{17}$$

Here, $u \in R^E$, $\bar{\rho}$, $\bar{\omega}$, $\bar{f}$ and $\bar{g}$ are as before and the $E \times (N - N_1)$ matrix $\mathcal{I}$ denotes the identity restricted to the boundary edge values.

Theorem 5.4. *Equations (14)-(17) have a unique solution $u \in U$.*

Proof. Consider the homogeneous problem $Fu = 0$ $C_0 u = 0$ $\mathcal{C}u = 0$ $\mathcal{I}u = 0$. In this case, $u \in W_0 \cap Z_0$ and by theorem 5.3 it follows that $u = 0$, giving uniqueness. Consequently, the matrix $[F^t\ C_0^t\ \mathcal{I}^t\ \mathcal{C}^t]$ which is of order $(E+1) \times E$ has rank E. The augmented matrix

$$\begin{bmatrix} F^t & C_0^t & \mathcal{I}^t & \mathcal{C}^t \\ \bar{\rho}^t & \bar{\omega}^t & \bar{f}^t & \bar{g}^t \end{bmatrix}^t$$

of order $(E+1) \times (E+1)$ has rank at most E. This follows by subtraction of the third block row from the sum of the first block of rows followed by use of the compatibility condition (3.12). Hence, existence follows. □.

A method for solving (14)-(17) by reducing them to potential equations can also be found using the results above including theorem 5.3. We can suppose without loss of generality that $\bar{f} = 0$, simply by substituting the known values of u into (14) and (15). These values do not appear in (16). We can also assume $\bar{g} = 0$ since it is trivial to find a solution of (16) and then modify u accordingly. Hence, it is only necessary to consider (14)-(17) with $\bar{f} = 0$ and $\bar{g} = 0$. That means $u \in \tilde{U}_0$. Now seek u as a sum $u^{(l)} + u^{(s)}$, where both of these are in $\tilde{U}_0$ and

$$\begin{aligned} Fu^{(l)} &= \bar{\rho} \\ C_0 u^{(l)} &= 0 \end{aligned} \tag{18}$$

and

$$\begin{aligned} Fu^{(s)} &= 0 \\ C_0 u^{(s)} &= \bar{\omega}. \end{aligned}$$

Consider the first set of equations. By theorem 5.1 we can write $u^{(l)} = S_0\phi$ and (18) then becomes

$$FS_0\phi = \bar{\rho}.$$

Taking account of the boundary conditions, this can be factored into

$$[S_0^t W_0^{1/2}][W_0^{1/2} S_0]\phi = \bar{\rho}.$$

The coefficient matrix is positive semidefinite since B_0 has rank $T-1$. Clearly, this reduction parallels a procedure for the continuous problem. The second set of equations can be solved by a similar approach. The details are given (for a different context) in section 7. These procedures reduce the equations (14)-(17) to the solution of positive semidefinite equations. Various iterative procedures for the solution of (14)-(17) turn out to be disguised iterations for these equations.

6 Error analysis. In this section we will estimate the error in approximating the solution $\mathbf{u}$ of the div-curl system (1)-(4) by the solution u of the covolume approximation (14)-(17).

To begin, we need the following result:

Lemma 6.1. *Assume that $v \in \mathcal{W}_0$ and that $u \in U_0$ and $Fu = 0$. Then $[u, v] = 0$.*

Proof. In this lemma we do not require that $u \in \tilde{U}_0$. By theorem 4.1,and using

$u|_\Gamma = 0$ we have $[u, v] = [u, S_0\phi] = [u, S\phi] = (Fu, \phi) = 0$ using lemma 5.1(1). □

Next, we introduce the following "mesh functions" $u^{(i)} \in U$ $i = 1, 2$ computed from the exact solution $\mathbf{u}$ of the div-curl system as follows:

$$u_k^{(1)} := \frac{1}{h_k} \int_{\sigma_k} \mathbf{u} \cdot \mathbf{n}\, ds \qquad k = 1, 2, \ldots, E \tag{19}$$

where σ_k is traversed positively, and $\mathbf{n}$ points to the right of σ_k, and

$$\begin{aligned} u_k^{(2)} &:= \frac{1}{h_k'} \int_{\sigma_k'} \mathbf{u} \cdot \mathbf{n}\, ds \qquad k = 1, 2, \ldots, E_1 \\ u_k^{(2)} &:= u_k^{(1)} \qquad k = E^{(1)} + 1, \ldots, E \end{aligned}$$

where σ_k' is traversed positively, and $\mathbf{n}$ points along σ_k'.

Now denoting $\epsilon^{(i)} := u - u^{(i)}$, $i = 1, 2$ we have

$$\begin{aligned} F\epsilon^{(1)} = 0 \quad \epsilon^{(1)} \in U_0 \\ C_0\epsilon^{(2)} = 0 \quad \epsilon^{(2)} \in \tilde{U}_0 \end{aligned}$$

Then by lemma 6.1

$$[\epsilon^{(1)}, \epsilon^{(2)}] = 0$$

and consequently, defining $\bar{u} := (u^{(1)} + u^{(2)})/2$, it follows that

$$\begin{aligned} [u - \bar{u}, u - \bar{u}] &= [\frac{1}{2}(\epsilon^{(1)} + \epsilon^{(2)}), \frac{1}{2}(\epsilon^{(1)} + \epsilon^{(2)})] \\ &= \frac{1}{4}[\epsilon^{(1)} - \epsilon^{(2)}, \epsilon^{(1)} - \epsilon^{(2)}] \\ &= \frac{1}{4}[u^{(1)} - u^{(2)}, u^{(1)} - u^{(2)}]. \end{aligned}$$

The right side is independent of u, while depending only on $\mathbf{u}$ so this gives a preliminary evaluation of the error. We can estimate the left side in terms of $u^{(1)}$, for example, by means of

$$\begin{aligned} \| u - \bar{u} \|_W &= \| u - u^{(1)} - (u^{(2)} - u^{(1)})/2 \|_W \\ &\geq \| u - u^{(1)} \|_W - \frac{1}{2} \| u^{(2)} - u^{(1)} \|_W \end{aligned}$$

so that the estimate becomes

$$\| u - u^{(1)} \|_W \leq \| u^{(2)} - u^{(1)} \|_W . \tag{20}$$

Evaluation of the right side of this proceeds as follows: referring to Figure 5 let K denote a kite shaped domain with perpendicular diagonals s and s'.

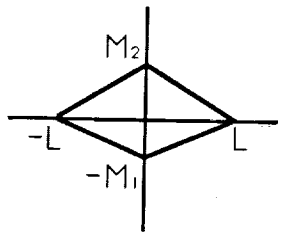

Figure 5:

We shall assume the diagonals are aligned with a Cartesian coordinate system intersecting at the origin O. Let the diagonal s on the x-axis extend from $x = -L$ to $x = L$ and let the diagonal s' on the y-axis extend from $y = -M_1$ to $y = M_2$. Define linear functionals $\mu^{(i)}$ $i = 1, 2$ on $\mathbf{H}^1(K)$ by

$$\begin{aligned} \mu^{(1)}(\mathbf{v}) &:= \frac{1}{2L}\int_{-L}^{L} v_2(x,0)\,dx \\ \mu^{(2)}(\mathbf{v}) &:= \frac{1}{M_1+M_2}\int_{-M_1}^{M_2} v_1(0,y)\,dy \end{aligned}$$

where $\mathbf{v} := (v_1, v_2) \in \mathbf{H}^1(K)$. By the trace theorem, $\mu^{(i)}(\cdot)$ $i = 1,2$ are bounded on $\mathbf{H}^1(K)$ and so is $\mu^{(1)}(\cdot) - \mu^{(2)}(\cdot)$. Also, if $\mathbf{v}$ is constant in K, then $(\mu^{(1)} - \mu^{(2)})(\mathbf{v}) = 0$. It follows that there exists a constant $C(K)$ such that

$$| (\mu^{(1)} - \mu^{(2)})(\mathbf{v}) | \leq C(K) \mid \mathbf{v} \mid_{1,K}$$

where $| \cdot |_{1,K}$ denotes the seminorm.

A standard scale change argument shows that $C(K)$ depends on the ratio

$$\max\left(\frac{M}{L}, \frac{L}{M}\right)$$

where $M :=| M_1 + M_2 |$. In terms of mesh geometry, for the kite associated with σ_k this becomes

$$\max\left(\frac{h_k}{h'_k}, \frac{h'_k}{h_k}\right).$$

Substitution into the right side of the error estimate now gives

$$\begin{aligned} \| u^{(2)} - u^{(1)} \|_W^2 &= \sum_k | (\mu^{(1)} - \mu^{(2)})(\mathbf{v}) |^2 | h_k h'_k | \\ &\leq \sum_k C|\mathbf{u}|^2_{1,K_k} \max(h_k^2, (h'_k)^2) \\ &\leq C \max(h^2, h'^2) \mid \mathbf{u} \mid^2_{1,\Omega} \end{aligned}$$

where $h := \max_k h_k$ and $h' := \max_k h'_k$. This proves:

Theorem 6.1. *Assume that* $\mathbf{u} \in \mathbf{H}^1(\Omega)$. *Then with* u *denoting the approximate solution and* $u^{(1)}$ *computed from (19), we have the estimate*

$$\| u - u^{(1)} \|_W \leq C \max(h, h') \mid \mathbf{u} \mid_{1,\Omega} .$$

Note that there is implicit dependence on the angles of the triangulation through the appearance of the dual mesh parameter h'.

This estimate can be improved for certain regular meshes. The key observation is that the functional $\mu^{(1)}(\cdot) - \mu^{(2)}(\cdot)$ vanishes on *linear* functions in K if the vertical diagonal in Figure 5 is also bisected. This will occur in a general triangulation iff all the triangles have the same circumradius. A complete characterization of such triangulations is not known. It certainly includes the standard uniform triangulation of the unit square, and the more symmetric triangulation in which each mesh square of the uniform rectangular mesh is subdivided by its diagonals. It also includes triangulations made of equilateral triangles. (The first two of these examples are brought within the covolume framework in section 10.) To exploit the mesh regularity, we assume now that $\mathbf{v} \in \mathbf{H}^2(K)$. Then it follows that

$$\mid (\mu^{(1)} - \mu^{(2)})(\mathbf{v}) \mid \leq C(K) \mid \mathbf{v} \mid_{2,K}$$

and the constant depends on

$$\max(\frac{L^3}{M}, \frac{M^3}{L}, ML).$$

Proceeding as above, we obtain for the regular meshes the estimate

$$\| u - u^{(1)} \|_W \leq C \max(h^2, (h')^2) \mid \mathbf{u} \mid_{2,\Omega} .$$

From the finite difference viewpoint, this means that the covolume scheme is second order accurate. The analysis strongly suggests that rapid changes in the circumradii of adjacent triangles should be avoided in practice. Similarly, we expect that meshes which vary smoothly in this sense will yield better accuracy. It would be possible to estimate the deviation from second order accuracy in terms of the change in adjacent circumradii, but we omit this.

7 Covolume solution of Poisson's equation. An interesting application of the stream function can be given. Consider the equation

$$-\Delta \Psi = \omega \qquad \Psi \in H^2(\Omega) \cap H_0^1(\Omega) \tag{21}$$

$$\Psi \mid_\Gamma = 0. \tag{22}$$

Integration over a covolume τ_j' gives

$$-\int_{\partial\tau_j'} \frac{\partial\Psi}{\partial n}\, ds = \int_{\tau_j'} \omega\, dx\, dy$$

and using the approximation $T\psi$ for $\frac{\partial\Psi}{\partial n}$, we get after approximation of the line integral

$$-C_0 T\psi = \bar{\omega}.$$

In more familiar notation, referring to Figure 6, a typical component of this equation is

$$-\sum_i h_i' \left(\frac{\psi_i - \psi_0}{h_i}\right) = \bar{\omega}_0. \tag{23}$$

Boundary conditions are used in the obvious way. We assume a locally equian-

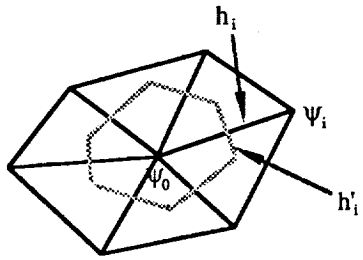

Figure 6:

gular triangulation. On rectangular meshes, and to a lesser extent on triangular ones, this approximation is well known.

Assembling the equations similar to (23), we obtain a linear system

$$\mathrm{K}\psi = \bar{\omega}$$

where K is of order $N_1 \times N_1$. K has the unexpected property of being the same as the piecewise linear finite element matrix for (21)-(22) on τ. That is, if λ_i $i = 1, 2, \ldots, N_1$ denote the standard piecewise linear basis functions for τ, then

$$\mathrm{K}_{ij} = \int_\Omega (\nabla\lambda_i)(\nabla\lambda_j)\, dx\, dy \qquad i, j = 1, 2, \ldots, N_1.$$

A proof may be found in [1]. Another proof could be based on the potentially useful factoring of K which follows by letting $G := H_0^{-1} D_0$. In terms of this we have

$$\mathrm{K} = G^t W_0 G.$$

This shows immediately, for example, that K is positive definite since D_0 has rank N_1.

A difference from the finite element formulation is apparent in the formation of the data vector $\bar{\omega}$. The components of this vector are formed by integration of ω against the characteristic functions of the covolumes. This is in contrast to the integration against the λ_i called for in exact finite element theory. It is possible that an error estimate for the covolume scheme could be derived from the finite element estimate by the usual techniques for handling quadrature formulas. On the other hand, it seems quite natural to obtain an estimate within the covolume framework. This can be done as follows. Define $u := T\Psi$. Then we have

$$\begin{aligned} Fu &= 0 \\ C_0 u &= \bar{\omega} \\ u\,|_\Gamma &= 0 \\ Cu &= \gamma_i \qquad i = 1, 2, ..., r \end{aligned}$$

where γ_i is computed as indicated. The exact solution of the analogous div-curl system is $\mathbf{u} = (u_1, u_2)$ where $u_1 = \partial_y \Psi$ and $u_2 = -\partial_x \Psi$. Based on $\mathbf{u}$ define $u^{(1)}$ by (19). Since $u^{(1)}\,|_\Gamma = 0$ and $Fu^{(1)} = 0$ by theorem 4.2 there exists $\psi^{(1)} \in R^N$ such that $u^{(1)} = T\psi^{(1)}$. Next, we have

Lemma 7.1.

$$\psi^{(1)}\,|_i = \Psi(x_i) \qquad i = 1, 2, \ldots, N.$$

Proof. By definition, integrating positively along σ_k, we have for $k = 1, 2, \ldots, E$

$$\begin{aligned} u_k^{(1)} &:= \frac{1}{h_k} \int_{\sigma_k} \mathbf{u} \cdot \mathbf{n}\, ds \\ &= \frac{1}{h_k} \int_{\sigma_k} (\partial_y \Psi, -\partial_x \Psi) \cdot \mathbf{n}\, ds \\ &= \frac{1}{h_k} \int_{\sigma_k} \frac{\partial \Psi}{\partial s}\, ds \\ &= (T\Psi)\,|_k \end{aligned}$$

so that $(T\Psi)\,|_k = (T\psi^{(1)})\,|_k$. Recalling that rank$(T)$=rank$(D)$=$N-1$, it follows that $\Psi(x_k)$ and $\psi(x_k)$ differ by a constant which can take to be zero. □

Define

$$a(\Phi, \Psi) := \int_\Omega (\nabla \Phi)(\nabla \Psi)\, dx\, dy \qquad \forall \Phi, \Psi \in H_0^1(\Omega).$$

The main result is:

Theorem 7.1. *Let $\hat{\psi}$ denote the piecewise linear interpolant of ψ the covolume approximation to Ψ. Then*

$$\| \hat{\psi} - \Psi \|_{1,\Omega} \leq C \max(h, h') \| \Psi \|_{2,\Omega} .$$

Proof. By theorem 6.1, we can write

$$\begin{aligned} \| u - u^{(1)} \|_W &= \| T\psi - T\psi^{(1)} \|_W \\ &\leq C \max(h, h') \| \Psi \|_{2,\Omega} \end{aligned}$$

and so

$$(C_0 T(\psi - \psi^{(1)}), \psi - \psi^{(1)}) \leq C[\max(h, h') \| \Psi \|_{2,\Omega}]^2.$$

By the lemma, denoting by $\hat{\Psi}$ the piecewise linear interpolant of Ψ on τ,

$$a(\hat{\psi} - \hat{\Psi}, \hat{\psi} - \hat{\Psi}) \leq C[\max(h, h') \| \Psi \|_{2,\Omega}]^2$$

and

$$a(\hat{\psi} - \Psi, \hat{\psi} - \Psi) \leq C[\max(h, h') \| \Psi \|_{2,\Omega}]^2 + a(\hat{\Psi} - \Psi, \hat{\Psi} - \Psi).$$

Using approximation theory it follows that

$$a(\hat{\psi} - \Psi, \hat{\psi} - \Psi) \leq C[\max(h, h') \| \Psi \|_{2,\Omega}]^2$$

and the result follows from Poincare-Friedrichs' inequality. □

Thus, the covolume scheme and the finite element scheme are of the same order in the $H^1(\Omega)$ norm.

8 Tangential Components. The discretizations of section 3 produce approximations to the velocity components normal to the triangle edges. Tangential field components are known in the directions of the comesh edges. This is a basic characteristic of the covolume method. But in many applications it is a vector field that is required and not merely sets of components. An example occurs in connection with approximating convection terms in viscous flow problems [7]. In this section we give an algorithm for computing a set of tangential components from a given set of normal components. In this way, a (discrete) vector field is obtained. The covolume scheme itself is not changed. Instead, the tangential components are found from the covolume solution in a "postprocessing" operation. Analysis of the error of the tangential approximations is also presented in this section.

We begin by noting that the three normal field components for a given triangle are too many to determine a constant field in the triangle. The following result

gives the compatibility condition for the three components to uniquely determine a constant field.

Lemma 8.1. *Given three normal components v_i, $i = 1,2,3$ on triangle sides with lengths h_i and corresponding unit outward normals $\mathbf{n}_i$ where $i = 1,2,3$ there exists a constant vector $\mathbf{u}$ such that*

$$\mathbf{u} \cdot \mathbf{n}_i = v_i \qquad i = 1,2,3 \tag{24}$$

iff the flux

$$v_1 h_1 + v_2 h_2 + v_3 h_3 = 0.$$

$\mathbf{u}$ *is unique.*

Proof. Equation (24) is a system of three equations for two components of $\mathbf{u}$. For nondegenerate triangles τ the coefficient matrix $A := (\mathbf{n}_i)_j$ clearly has rank 2, so it follows that $\dim N(A^t) = 1$. Now the equation

$$Aw = 0$$

certainly has the solution $w = (h_1, h_2, h_3)$, since

$$0 = \int_\tau \nabla(1)\, dx\, dy = \int_{\partial\tau} \mathbf{n}\, ds = \mathbf{n}_1 h_1 + \mathbf{n}_2 h_2 + \mathbf{n}_3 h_3.$$

Hence, (24) will be solvable uniquely iff

$$v_1 h_1 + v_2 h_2 + v_3 h_3 = 0$$

which is what we wanted to show. □

From this lemma it follows that if $Fu = 0$, then we can construct a piecewise constant vector field $\mathbf{u}$ on τ whose (continuous) normal components are given by u. An easy way to compute a tangential component along an edge of the triangulation is to average the tangential components of the constant fields in the triangles sharing the edge. The remaining problem is then to construct the piecewise constant field when the flux is nonzero and lemma 8.1 does not apply. There is no unique way to do this. For example, we can take any pair of normal components and designate them as the respective components of the sought vector in a triangle. This procedure will be used. Denoting the kite areas associated with the triangle by $K_1 \geq K_2 \geq K_3$, we choose the corresponding components u_1 and u_2 associated with the largest and second largest kite areas to define the vector.

To compute a constant interpolating field $\mathbf{u}_I$, let $\vec{u} := (u_1, u_2)$ and define $\cos\theta := \mathbf{n}_1 \cdot \mathbf{n}_2$. Representing $\mathbf{u}_I := \alpha_1 \mathbf{n}_1 + \alpha_2 \mathbf{n}_2$ gives the equations

$$\begin{pmatrix} 1 & \cos\theta \\ \cos\theta & 1 \end{pmatrix} \begin{pmatrix} \alpha_1 \\ \alpha_2 \end{pmatrix} = \begin{pmatrix} u_1 \\ u_2 \end{pmatrix} \tag{25}$$

which uniquely determine α_1, α_2. It can be checked from this representation that

$$\mathbf{u}_I \cdot \mathbf{u}_I \leq \frac{2}{\sin^2\theta}\,\vec{u}\cdot\vec{u}, \tag{26}$$

a result we will use below.

Interpolation of the $\mathbf{u}_I$'s across the common edge of their triangles is also subject to a certain amount of arbitrariness. One possibility is to use the vector from one of the triangles and ignore the other. Another is to weight the vectors equally, while a third is to use full linear interpolation. In this last case, it is necessary to assign a localization of the vectors. The most natural choice is to attach each $\mathbf{u}_I$ to the circumcenter of its triangle. To justify this, we can observe that the two directions from which $\mathbf{u}_I$ is made indeed pass through the circumcenter. The line joining the circumcenters is divided in a certain ratio by the common edge of the triangles which determines the interpolation weights in the usual way. Note that if one of the triangles is obtuse, this becomes a linear extrapolation. Each of these methods corresponds to a weighting of the form $\lambda_1\mathbf{u}_I^{(1)} + \lambda_2\mathbf{u}_I^{(2)}$ in which $\lambda_1 + \lambda_2 = 1$. Some situations suggest other weightings to use. At boundaries in particular, a $(1,0)$ weighting is required. In other cases the weights can vary from edge to edge.

Next, we will estimate the error of this tangential approximation scheme. The interpolated vector for the k^{th} edge has the form

$$\mathbf{w}^{(k)} := \lambda_1^{(k_1)}\mathbf{u}_I^{(k_1)} + \lambda_2^{(k_2)}\mathbf{u}_I^{(k_2)}$$

where the superscripts (k_1), (k_2) denote the two triangles on each side of the k^{th} edge. The tangential component of this is just $\mathbf{t}^{(k)}\cdot\mathbf{w}^{(k)}$. For $u \in U$, let $\mathcal{T}u \in U$ denote the mapping to the tangential components generated in this way.

A parameter which will appear in the estimate is the ratio $\sqrt{K_1^{(j)}/K_2^{(j)}} =: \delta^{(k)}$, where $K^{(j)}$ are the kite areas for τ_j. We will define $\delta := \max_j(\delta^{(j)})$. This quantity will be estimated later. Also we will define $\Theta := \min_m(|\sin\theta^{(m)}|)$ where $\theta^{(m)}$ corresponds to the angle in (25) above and the minimum is over the triangles. In addition to these we will denote by λ the maximum absolute interpolation coefficient: $\lambda := \max_k(|\lambda_1^{(k)}|, |\lambda_2^{(k)}|)$. The next result will be required below:

Lemma 8.1. *The following bound on $\mathcal{T}$ holds:*

$$\|\mathcal{T}u\|_W \leq \frac{4\delta\lambda}{\Theta}\,\|u\|_W \qquad \forall\, u \in U.$$

Proof. Let $K^{(k)}$ denote the kite area on the edge σ_k. Then since

$$|\mathbf{t}^{(k)}\cdot\mathbf{w}^{(k)}|^2 \leq 2\lambda^2(\|\mathbf{u}_I^{(k_1)}\|_{l^2}^2 + \|\mathbf{u}_I^{(k_2)}\|_{l^2}^2)$$

we have, using (26)

$$\begin{aligned}\sum_k |(\mathcal{T}u)_k|^2 K^{(k)} &= \sum_k |\mathbf{t}^{(k)} \cdot \mathbf{w}^{(k)}|^2 K^{(k)} \\ &\leq \frac{4\lambda^2}{\Theta^2} \sum_k (|\vec{u}^{(k_1)}|^2 + |\vec{u}^{(k_2)}|^2) K^{(k)}.\end{aligned}$$

Also

$$\begin{aligned}|\vec{u}^{(k_1)}|^2 K^{(k)} &= [(u_1^{(k_1)})^2 + (u_2^{(k_1)})^2] K^{(k)} \\ &\leq \delta^2 [(u_1^{(k_1)})^2 K_1^{(k_1)} + (u_2^{(k_1)})^2 K_2^{(k_1)}]\end{aligned}$$

with a similar bound for $|\vec{u}^{(k_2)}|^2 K^{(k)}$. Noting that each product appears at most four times and substituting these into the previous inequality gives the result. □

Next, let $\mathbf{u} \in \mathbf{H}^1(\Omega)$, and define $u^{(1)}$ by (19). In addition, let $v^{(1)}$ be defined by

$$v_k^{(1)} := \frac{1}{h_k} \int_{\sigma_k} \mathbf{t} \cdot \mathbf{u}\, ds \qquad k = 1, 2, ..., E \tag{27}$$

where σ_k is traversed positively and $\mathbf{t}$ denotes the unit tangent along σ_k. Now we have:

Lemma 8.2. *The estimate*

$$\|v^{(1)} - \mathcal{T}u^{(1)}\|_W \leq \frac{C\lambda}{\Theta} \max(h, h') \|\mathbf{u}\|_{1,\Omega}$$

holds.

Proof. Let σ_k denote an edge of $\tau_j \in \tau$. The functional

$$\nu_j(\mathbf{u}) := (v_k^{(1)} - \mathbf{t}_k \cdot \mathbf{u}_I^{(j)})$$

is linear, bounded on $\vec{\mathbf{H}}^1(\tau_j)$ by the trace theorem, vanishes on constant $\mathbf{u}$, and so has the estimate

$$|\nu_j(\mathbf{u})| \leq C(\tau_j) |\mathbf{u}|_{1,\tau_j}.$$

By the usual mapping to a reference element [3] it follows that

$$C(\tau_j) \leq \frac{C}{\Theta}.$$

Following the notation of the previous proof, using $\lambda_1 + \lambda_2 = 1$ we have

$$\begin{aligned}(v^{(1)} - \mathcal{T}u^{(1)})_k &\leq \lambda(|\nu_{k_1}(\mathbf{u})| + |\nu_{k_2}(\mathbf{u})| \\ &\leq \frac{C\lambda}{\Theta}(|\mathbf{u}|_{1,\tau_{k_1}} + |\mathbf{u}|_{1,\tau_{k_2}}).\end{aligned}$$

and consequently with a modified constant C,

$$\sum_k |(v^{(1)} - \mathcal{T}u^{(1)})_k|^2 K^k \leq (\frac{C\lambda}{\Theta})^2 \max_k(K^{(k)}) \sum_j |\mathbf{u}|^2_{1,\tau_j}$$

which is equivalent to the required result. □

Combining lemmas 8.1 and 8.2 now gives:

Lemma 8.3. *Let $u \in U$ denote the covolume approximation to $\mathbf{u} \in \mathbf{H}^1(\Omega)$ estimated in theorem 6.1 and let $\mathcal{T}u$ denote the approximate tangential components. Then the estimate*

$$\|v^{(1)} - \mathcal{T}u\|_W \leq \frac{C\lambda\delta}{\Theta} max\,(h,\, h')\|\mathbf{u}\|_{1,\Omega}$$

holds where $v^{(1)}$ is defined by (27).

Proof. It is only necessary to observe that

$$\|v^{(1)} - \mathcal{T}u\|_W \leq \|v^{(1)} - \mathcal{T}u^{(1)}\|_W + \|\mathcal{T}(u - u^{(1)})\|_W$$

and to use lemma 8.2 on the first term and lemma 8.1 and theorem 6.1 on the second. □

We may now construct the discrete vector field $\mathbf{u}_{cv} := (u, \mathcal{T}u) \in U \times U$ and regard it as a covolume approximation to $\mathbf{u}$ the solution of the div-curl system (1)-(4). The error estimate for $\|(u - u^{(1)}, \mathcal{T}u - v^{(1)})\|^2_W := \|u - u^{(1)}\|^2_W + \|\mathcal{T}u - v^{(1)}\|^2_W$ follows immediately. Defining $\mathbf{u}^{(1)} := (u^{(1)}, v^{(1)})$ we summarize with

Theorem 8.1. *The covolume approximation $\mathbf{u}^{(1)}$ satisfies*

$$\|\mathbf{u}_{cv} - \mathbf{u}^{(1)}\|_W \leq \frac{C\lambda\delta}{\Theta} \max\,(h,\, h')\|\mathbf{u}\|_{1,\Omega}$$

where Θ denotes $\min_m |sin\,\theta_m|$, θ_m denoting the angles of the triangles in τ, λ denotes the largest absolute interpolation coefficient, and δ^2 denotes the largest kite ratio for triangles in the triangulation.

Proof. This is simply a question of applying the definition of the norm on the left and theorem 6.1 and lemma 8.3. □.

We can make this bound more explicit for acute angled triangulations. In that case, we have $\lambda \leq 1$. For any acute angled triangle $\tau_j \in \tau$, let $A_1^{(j)} \geq A_2^{(j)} \geq A_3^{(j)} \geq 0$ denote the areas of the three triangles formed when the circumcenter is joined to the vertices. Thus $A_i^{(j)}/|\tau_j|$ are the barycentric coordinates of the circumcenter. Obviously, $A_1^{(j)} \geq |\tau_j|/3$. A calculation shows that $A_1^{(j)} \leq 2A_2^{(j)}$. We will also use the area ratio of the triangulation defined by

$$r_\tau := \max_{i,j} \frac{|\tau_i|}{|\tau_j|} \qquad (\tau_i,\, \tau_j \text{ adjacent}).$$

Note that this ratio is formed for *adjacent* triangles only.

Denote the kite areas of τ_j by $K_1^{(j)} \geq K_2^{(j)} \geq K_3^{(j)} > 0$ (since $h'_k > 0$). Below, we will use the fact that for acute triangles we always have $A_2^{(j)} \leq K_2^{(j)}$. This follows since the maximal property of $K_2^{(j)}$ ensures that it is always at least as large as the $A^{(j)}$ which are not part of $K_1^{(j)}$. But at least one of these two $A^{(j)}$ must be at least equal to $A_2^{(j)}$, so the above property does hold. It follows that

$$\begin{aligned} K_1(\tau_j) &= h_k h'_k/2 \\ &\leq A_1(\tau_j) + r_\tau |\tau_j| \\ &\leq 2A_2(\tau_j) + r_\tau 3A_1(\tau_j) \\ &\leq 2K_2(\tau_j) + r_\tau 3 \cdot 2K_2(\tau_j) \\ &\leq 8r_\tau K_2(\tau_j). \end{aligned}$$

This shows that we can take $\delta = \sqrt{8r_\tau}$. It would of course be possible to bound r_τ in terms of mesh lengths and Θ but we prefer not to do this. Instead, making use of this value for δ in theorem 8.1 now gives the estimate

$$\|\mathbf{u}_{cv} - \mathbf{u}^{(1)}\|_W \leq \frac{C\sqrt{r_\tau}}{\Theta} \max(h, h') \|\mathbf{u}\|_{1,\Omega}.$$

This is valid for acute triangulations.

Estimating λ and δ is more difficult when there are obtuse triangles. The problem is associated with h'_k/h_k values which approach zero. This will not be discussed further here, but section 9 has some related information.

9 Comments on rectangular meshes. The earlier results have been obtained under the assumption that all $h'_k > 0$. This is equivalent to assuming that circumcenters of adjacent triangles are distinct. Now we will briefly summarize the necessary changes for the contrary case. The previous results continue to hold with some slight changes.

Coincident circumcenters will occur if the triangulation contains a cyclic quadrilateral Q. The distance between the circumcenters of the two triangles making Q is $h' := 0$. There is no change in the definition of the covolumes, and the discrete circulation equations (9) continue to approximate the continuous ones (2). Note that the normal component for the diagonal does not appear in the circulation equations. The flux equations are also unchanged by the existence of Q, but the diagonal component does appear in them. A problem shows up in the analysis, since the kite area for the diagonal is zero and consequently $\|\cdot\|_W$ is now merely a seminorm. This inconvenience is easily removed by a slight modification of the equations: we simply add the two flux equations associated with Q. The diagonal component does not appear in the resulting sum.

In this way, the number of equations is reduced by one and so is the number of equations.

More directly, we can modify the triangulation by deleting the diagonals of all cyclic quadrilaterals. Circumcenters are well defined for each of the resulting mesh figures. Flux and circulation equations are written in the obvious way. Euler's formula, lemma 2.1 is still true and there will be a single consistency condition analogous to (5). The effect of this modification is to remove the dual edges which have $h' = 0$. With these gone, we can prove the key theorem 5.1. which requires the existence of $(h')^{-1}$. Still defining the kite areas by joining circumcenters of mesh figures to their vertices, the results in sections 6-7 follow essentially verbatim.

These observations apply particularly to cartesian rectangular meshes. Normal to vertical (horizontal) mesh segments we have horizontal (vertical) field components. Flux equations are written for mesh rectangles, and circulation equations for the dual mesh rectangles around the mesh points. The two potentials ϕ and ψ are defined respectively at the mesh cell circumcenters and the mesh points themselves. The mesh pair is the same as the usual staggered mesh system found in fluid flow discretizations. Error estimation of this scheme is given at the end of section 6, where second order accuracy is demonstrated. The scheme itself is advocated in [2].

There are occasions when rectangular and triangular meshes can be usefully combined. This is especially true when highly stretched meshes must be used. In regions where stretching is necessary, rectangular mesh cells can be used in place of triangles. This might be helpful in calculations involving boundary and other kinds of layers.

A situation related to the above occurs when some h'_k/h_k is small, but positive. Although, in a sense, this is inconsequential from the analytical viewpoint, in finite precision environments instabilities could result. The three dimensional case is worse in this respect, because there is more opportunity for degeneracy. In practice, it should be satisfactory to merely set to zero those h' for which h'_k/h_k is below some threshold and proceed as indicated above. This does introduce some extra error, but by a suitable choice of the threshold it should be within the discretization error.

10 Mixed boundary conditions. In this section, we will extend the earlier results to boundary conditions which are partly normal and partly tangential. The technique will be illustrated for the simply connected problem. If required, multiply connected cases can be handled by direct extension of the method already used in earlier sections.

We consider in the simply connected polygonal domain Ω the system

$$\operatorname{div} \mathbf{u} = \rho \qquad \text{in } \Omega \tag{28}$$

$$\operatorname{curl} \mathbf{u} = \omega \qquad \text{in } \Omega \tag{29}$$

$$\mathbf{u} \cdot \mathbf{n} = f \qquad \text{on } \Gamma_n \tag{30}$$

$$\mathbf{u} \cdot \mathbf{t} = g \qquad \text{on } \Gamma_t \tag{31}$$

where $\Gamma = \Gamma_n \cup \Gamma_t$ and neither part has zero measure. For illustration,we can assume that Γ is divided into two continuous parts Γ_n and Γ_t each with nonzero length. We assume that $\rho \in L^2(\Omega)$, $\omega \in L^2(\Omega)$ and $f \in H^{1/2}(\Gamma)$ and that the system has a unique solution $\mathbf{u} \in \mathbf{H}^1(\Omega)$

Discretization of (28)-(31) follows section 3, except that (10) is applied only to boundary edges on Γ_n. Here and below, it is assumed that nodes of the triangulation always separate Γ_n and Γ_t and that, conventionally, the separating nodes belong to Γ_t. Boundary edges of τ which are in Γ_n are labelled $E_1 + 1, ..., E_2$ and boundary edges in Γ_t are labelled $E_2 + 1, ..., E$. Then in place of (10) we have

$$u_k = \frac{1}{h_k} \int_{\sigma_k} f \, ds \qquad k = E_1 + 1, \ldots, E_2.$$

To complement the boundary conditions, some boundary circulation equations are used. The derivation of these equations will be illustrated using Figure 7. ABC is part of Γ_t and the boundary covolume τ'_B associated with the node at

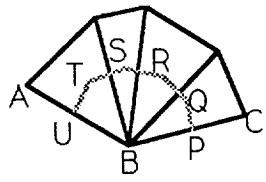

Figure 7:

B is shown. The orientation conventions are unchanged. Define

$$v_{AB} := \frac{1}{|AB|} \int_{AB} g \, ds$$

and

$$v_{BC} := \frac{1}{|BC|} \int_{BC} g \, ds,$$

where $\vec{AB}$ and $\vec{BC}$ are the positive directions. The circulation equation for $\partial\tau'_B$ is approximated by

$$\sum_{\partial\tau'_B} u_i h'_i + \frac{1}{2} v_{AB} h_{AB} + \frac{1}{2} v_{BC} h_{BC} = \int_{\tau'_B} \omega \, dx \, dy \tag{32}$$

and a similar equation is used for each boundary covolume associated with a node strictly interior to Γ_t. It is always assumed, without explicit mention, that h is sufficiently small for Γ_t to contain at least one strictly interior node. This assumption is essential for what follows. If it is not satisfied, then we are essentially in the situation of the previous sections as far as the discretization is concerned.

The system of equations which results may be written as

$$Fu = \bar{\rho} \tag{33}$$

$$C_b u = \bar{\omega} - \bar{g} \tag{34}$$

$$u|_\Gamma = \bar{f} \tag{35}$$

where $\bar{g}$ is found from the terms involving the tangential boundary function in equations like (32) and C_b has no explicit dependence on the lengths of the boundary edges.

The number of nodes interior to Γ_t is $E - E_2$ and the number of edges is therefore $E - E_2 - 1$. In all, the number of equations is

$$\begin{aligned} T + N_1 + (E - E_2 - 1) + (E_2 - E_1) &= T + N - 1 \\ &= E \end{aligned}$$

by lemma 2.1. This time, unlike the earlier situation the number of equations and unknowns are equal.

Now we will prove that the solution of the linear system is unique. For this, we will generalize the Helmholtz type theorem 5.3 to cover the new boundary conditions. It is necessary first to have results analogous to theorems 4.1 and 5.1.

Recalling the definition of the matrix D in section 4, let D_b denote the restriction of D to $\{x_i;\ x_i \in \Omega \cup \Gamma_t\}$, and let B_b denote B with columns $E_2 + 1, \ldots, E$ deleted. Thus, $\dim R(B_b) = E_1 + E - E_2 =: E'$.

Theorem 10.1 *Let Ω be simply connected and assume that $v \in R^{E'}$. Then there exists $\phi \in R^T$ such that $v = B_b\phi$ iff $D_b^t v = 0$.*

Proof. The proof of this follows closely the proof of theorem 4.1 and we shall omit most of the details. We have to solve

$$B_b\phi = v.$$

That

$$B_b^t D_b \psi = 0$$

follows from the easily proved relation $B^t D\psi = 0$. Also, rank $(D_b) = N'$, where N' denotes the number of interior nodes plus nodes on Γ_t. In addition,

$$\dim N(B_b^t) = E' - T.$$

Counting and use of lemma 2.1 shows that $N' = E' - T$ so the result follows. □

Now we have that $C_b u = 0$ iff $D_b^t H' u = 0$. Define $S_b := (H')^{-1} B_b$ (denoting the restriction of $(H')^{-1}$ to $R(B_b)$ by the same symbol). It follows that $C_b u = 0$ iff $u = S_b \phi$ for some $\phi \in R^T$.

Next, define

$$\begin{aligned} U_0' &:= \{u \in R^E; u|_{\Gamma_t} = 0\} \\ W_0' &:= \{u \in U_0'; C_b u = 0\} \\ Z_0' &:= \{u \in U_0'; Fu = 0\}. \end{aligned}$$

Theorem 10.2 *Assume that Ω is simply connected. Then U_0' has the decomposition*

$$U_0' = W_0' \oplus Z_0'$$

which is orthogonal relative to $[\cdot, \cdot]$.

Proof. $w \in W_0'$ implies $[u, w] = [u, S_b\phi] = [u, S\phi] = (Fu, \phi)$. Hence, $[u, w] = 0$ for all $w \in W_0'$ implies that $Fu = 0$. The rest of the argument is as before. □

Existence and uniqueness for the discrete system follows directly, since if u is a solution of the homogeneous system we have $u \in W_0' \cap Z_0' = 0$. Existence follows from uniqueness since the coefficient matrix is square.

It remains to estimate the error of this approximation. The method is similar to section 7 with some small modificaions. We define $u^{(1)}$ just as in (19). Corresponding to $u^{(2)}$ we define a very slightly different function, still denoted by $u^{(2)}$ as follows:

$$\begin{aligned} u_k^{(2)} &:= \frac{1}{h_k'} \int_{\sigma_k'} \mathbf{u} \cdot \mathbf{n}\, ds \qquad k = 1, 2, \ldots, E_1 \qquad k = E_2 + 1, \ldots, E \\ u_k^{(2)} &:= u_k^{(1)} \qquad k = E^{(1)} + 1, \ldots, E_2. \end{aligned}$$

The edges $\sigma_k \quad k = E_2 + 1, ..., E$ are in Γ_t ; each of the coedges σ_k' extends from σ_k's midpoint to the circumcenter of the triangle containing σ_k, exemplified by PQ and TU in Figure 7. As before, define $\epsilon^{(i)} = u - u^{(i)}$ $i = 1, 2$. Then

$$\begin{aligned} F\epsilon^{(1)} &= 0 \quad \epsilon^{(1)} \in Z_0' \\ C_b\epsilon^{(2)} &= 0 \quad \epsilon^{(2)} \in W_0' \end{aligned}$$

and $[\epsilon^{(1)}, \epsilon^{(2)}] = 0$ by theorem 10.2. Following the method of section 6, we obtain, corresponding to (20)

$$\|u - u^{(1)}\|_W \leq \|u^{(2)} - u^{(1)}\|_W.$$

The right side can be estimated as before, except that now there will be a contribution to the norm from the boundary segments along Γ_t. The earlier estimation technique works here too, and is especially simple if each coedge associated with Γ_t lies wholly in Ω. This will certainly be the case, for example, if the boundary triangles are acute angled, since then the coedges will lie inside the triangles themselves. That is the simplest case. We summarize this discussion with:

Theorem 10.3 *For the equations (28)-(31) and their discretization (33)-(35), we have the estimate*

$$\|u - u^{(1)}\|_W \leq C \max(h, h')|u|_{1,\Omega}.$$

So far, we have considered the purely normal boundary condition and the mixed boundary condition. For the purely tangential case the simplest approach seems to be to use tangential field components in place of the normal ones used in sections 2-6. The circulation equations are formed using the triangle boundaries and the flux equations are formed using the covolume boundaries. It is apparent that this method gives a natural dual to the earlier one. We will not go into the details here, but an almost verbatim development of the theory can be carried out. This includes most of the results of sections 2-6. The main difference is to exchange the roles of ϕ and ψ. This duality is strongly reminiscent of complex variable theory. In fact, a similar connection was developed in [5]. The results given above provide useful tools for the analysis of that scheme.

References

[1] C.Börgers, C. Peskin. A Lagrangian Method Based on the Voronoi Diagram for the Incompressible Navier-Stokes Equations on a Periodic Domain. Proc. Intnl. Conf. on Free Lagrange Methods, ed. M. J. Fritts et al. Lecture Notes in Physics v. 238 Springer Verlag (1985)

[2] A. Brandt, N. Dinar. Multigrid Solutions to Elliptic Flow Problems; in Numerical Methods for Partial Differential Equations, ed. S. V. Parter, Academic Press (1979)

[3] P. Ciarlet. The Finite Element Method for Elliptic Problems, North Holland (1977)

[4] S. Choudhury, R. A. Nicolaides. Discretization of incompressible vorticity-velocity equations on triangular meshes. (to appear in Intnl. Jnl. Num. Meth. Fluid Dynamics)

[5] R. Duffin. Potential Theory on a Rhombic Lattice. Jnl. Comb. Th. 5, (1968) p258

[6] V. Girault, P-A. Raviart. Finite Element Methods for Navier-Stokes Equations, Springer-Verlag, (1986)

[7] R. A. Nicolaides. Flow Discretization by Complementary Volume Techniques. AIAA Paper 89-1978. Proceedings of the 9th AIAA CFD Meeting, Buffalo, New York, June 1989.

[8] R. Sibson. Locally Equiangular Triangulations. Computer Jnl. 21, (1978) p243

[9] W. Wendland. Elliptic Systems in the Plane, Pitman, (1979)

[10] S. Wong, Z. Cendes. Combined Finite Element-Modal Solution of Three Dimensional Eddy Current Problems. IEEE Trans. on Magnetics 24, (1988) p2685

NASA
National Aeronautics and Space Administration

Report Documentation Page

1. Report No.	2. Government Accession No.	3. Recipient's Catalog No.
NASA CR-181935 ICASE Report No. 89-76		

4. Title and Subtitle	5. Report Date
DIRECT DISCRETIZATION OF PLANAR div-curl PROBLEMS	October 1989
	6. Performing Organization Code

7. Author(s)	8. Performing Organization Report No.
R. A. Nicolaides	89-76
	10. Work Unit No.
	505-90-21-01

9. Performing Organization Name and Address	11. Contract or Grant No.
Institute for Computer Applications in Science and Engineering Mail Stop 132C, NASA Langley Research Center Hampton, VA 23665-5225	NAS1-18605
	13. Type of Report and Period Covered
12. Sponsoring Agency Name and Address	Contractor Report
National Aeronautics and Space Administration Langley Research Center Hampton, VA 23665-5225	14. Sponsoring Agency Code

15. Supplementary Notes

SIAM Journel

Langley Technical Monitor:
Richard W. Barnwell

Final Report

16. Abstract

A control volume method is proposed for planar div-curl systems. The method is independent of potential and least squares formulations, and works directly with the div-curl system. The novelty of the technique lies in its use of a single local vector field component and two control volumes rather than the other way round. A discrete vector field theory comes quite naturally from this idea and is developed in the paper. Error estimates are proved for the method, and other ramifications investigated.

17. Key Words (Suggested by Author(s))	18. Distribution Statement
finite difference methods, finite difference elements, div-curl equations	64 - Numerical Analysis Unclassified - Unlimited

19. Security Classif. (of this report)	20. Security Classif. (of this page)	21. No. of pages	22. Price
Unclassified	Unclassified	31	A03

NASA FORM 1626 OCT 86